

Biogenic and Synthetic Polyamines Bind Cationic Dendrimers

Jean-Sebastian Mandeville¹, Phillipe Bourassa¹, Thekkumkattil John Thomas^{2,3}, Heidar-Ali Tajmir-Riahi^{1*}

1 Département de Chimie-Biologie, Université du Québec à Trois-Rivières, Trois-Rivières, Québec, Canada, **2** Department of Medicine, University of Medicine and Dentistry of New Jersey-Robert Wood Johnson Medical School, New Brunswick, New Jersey, United States of America, **3** The Cancer Institute of New Jersey, University of Medicine and Dentistry of New Jersey, Robert Wood Johnson Medical School, New Brunswick, New Jersey, United States of America

Abstract

Biogenic polyamines are essential for cell growth and differentiation, while polyamine analogues exert antitumor activity in multiple experimental model systems, including breast and lung cancer. Dendrimers are widely used for drug delivery *in vitro* and *in vivo*. We report the bindings of biogenic polyamines, spermine (spm), and spermidine (spmd), and their synthetic analogues, 3,7,11,15-tetrazaheptadecane.4HCl (BE-333) and 3,7,11,15,19-pentazahenicosane.5HCl (BE-3333) to dendrimers of different compositions, mPEG-PAMAM (G3), mPEG-PAMAM (G4) and PAMAM (G4). FTIR and UV-visible spectroscopic methods as well as molecular modeling were used to analyze polyamine binding mode, the binding constant and the effects of polyamine complexation on dendrimer stability and conformation. Structural analysis showed that polyamines bound dendrimers through both hydrophobic and hydrophilic contacts with overall binding constants of $K_{\text{spm-mPEG-G3}} = 7.6 \times 10^4 \text{ M}^{-1}$, $K_{\text{spm-mPEG-PAMAM-G4}} = 4.6 \times 10^4 \text{ M}^{-1}$, $K_{\text{spm-PAMAM-G4}} = 6.6 \times 10^4 \text{ M}^{-1}$, $K_{\text{spmd-mPEG-G3}} = 1.0 \times 10^5 \text{ M}^{-1}$, $K_{\text{spmd-mPEG-PAMAM-G4}} = 5.5 \times 10^4 \text{ M}^{-1}$, $K_{\text{spmd-PAMAM-G4}} = 9.2 \times 10^4 \text{ M}^{-1}$, $K_{\text{BE-333-mPEG-G3}} = 4.2 \times 10^4 \text{ M}^{-1}$, $K_{\text{BE-333-mPEG-PAMAM-G4}} = 3.2 \times 10^4 \text{ M}^{-1}$, $K_{\text{BE-333-PAMAM-G4}} = 3.6 \times 10^4 \text{ M}^{-1}$, $K_{\text{BE-3333-mPEG-G3}} = 2.2 \times 10^4 \text{ M}^{-1}$, $K_{\text{BE-3333-mPEG-PAMAM-G4}} = 2.4 \times 10^4 \text{ M}^{-1}$, $K_{\text{BE-3333-PAMAM-G4}} = 2.3 \times 10^4 \text{ M}^{-1}$. Biogenic polyamines showed stronger affinity toward dendrimers than those of synthetic polyamines, while weaker interaction was observed as polyamine cationic charges increased. The free binding energies calculated from docking studies were: -3.2 (spermine), -3.5 (spermidine) and -3.03 (BE-3333) kcal/mol, with the following order of binding affinity: spermidine-PAMAM-G4 > spermine-PAMAM-G4 > BE-3333-PAMAM-G4 consistent with spectroscopic data. Our results suggest that dendrimers can act as carrier vehicles for delivering antitumor polyamine analogues to target tissues.

Citation: Mandeville J-S, Bourassa P, Thomas TJ, Tajmir-Riahi H-A (2012) Biogenic and Synthetic Polyamines Bind Cationic Dendrimers. PLoS ONE 7(4): e36087. doi:10.1371/journal.pone.0036087

Editor: Laurent Kreplak, Dalhousie University, Canada

Received: February 21, 2012; **Accepted:** March 26, 2012; **Published:** April 27, 2012

Copyright: © 2012 Mandeville et al. This is an open-access article distributed under the terms of the Creative Commons Attribution License, which permits unrestricted use, distribution, and reproduction in any medium, provided the original author and source are credited.

Funding: The authors have no funding or support to report.

Competing Interests: The authors have declared that no competing interests exist.

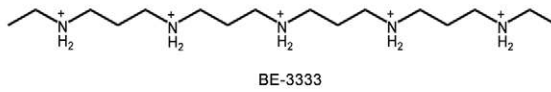
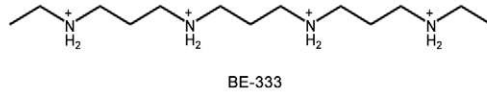
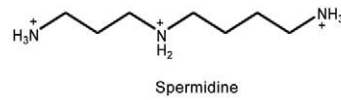
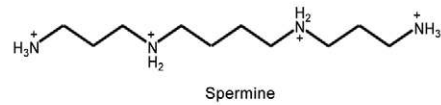
* E-mail: tajmirri@uqtr.ca

Introduction

Polyamine analogues (Fig. 1) exert antitumor activity in multiple experimental model systems, including breast and lung cancer models and they are being used in clinical trials [1–5]. Synthetic polyamines can mimic some of the self-regulatory functions of biogenic polyamines but are unable to substitute for natural polyamines in their growth promoting role [6–13]. Natural polyamines are ubiquitous cellular cations and are involved in cell growth and differentiation [14]. They are capable of modulating gene expression and enzyme activities, activation of DNA synthesis, and facilitating protein-DNA interactions [13–20]. Even though interactions of biogenic and synthetic polyamines with DNA and RNA are well characterized [21–25], little is known about their interaction with therapeutically important synthetic polymers, such as dendrimers [26].

Synthetic polymers with a specific shape and size play important roles in the development of modern drug and gene delivery systems [27–29]. Dendrimers are unique synthetic macromolecules of nanometer dimensions with a highly branched structure and globular shape [29,30]. Among dendrimers, polyamidoamine

(PAMAM) dendrimers (Fig. 1) have received most attention as potential gene and drug delivery systems [31–33]. Several attempts have been made to design different dendrimers as drug carriers [34]. For example, anticancer fluorouracil drug was attached to dendrimers with a cyclic core [35], while dendrimers with poly(ethylene glycol) grafts were used to encapsulate antitumor drugs adriamycin and methotrexate [36]. Similarly, it has been shown that a poly(propyleneimine) dendrimers endcapped with 64 L-phenylalanine encapsulated nearly 4 molecules of Bengal Rose for every dendritic molecule [37]. Since dendrimers have a large number of terminal groups to which drug molecules can be attached, they can carry drug molecules with a high efficiency. They contain several binding sites for hydrophobic, hydrophilic, cationic and anionic drugs. In developing dendrimers for drug delivery, it is important to use dendrimers with low toxicity and excellent biocompatibility. However, dendrimers such as PAMAM (polyamidoamine) and polypropyleneimine (PPI) are toxic. It has been demonstrated that modification of the amino groups on the periphery of dendrimers with poly(ethylene glycol) could reduce toxicity and increase biocompatibility [38–40]. Poly(ethylene glycol) is nontoxic, nonimmunogenic and water soluble, and its



Polyamines

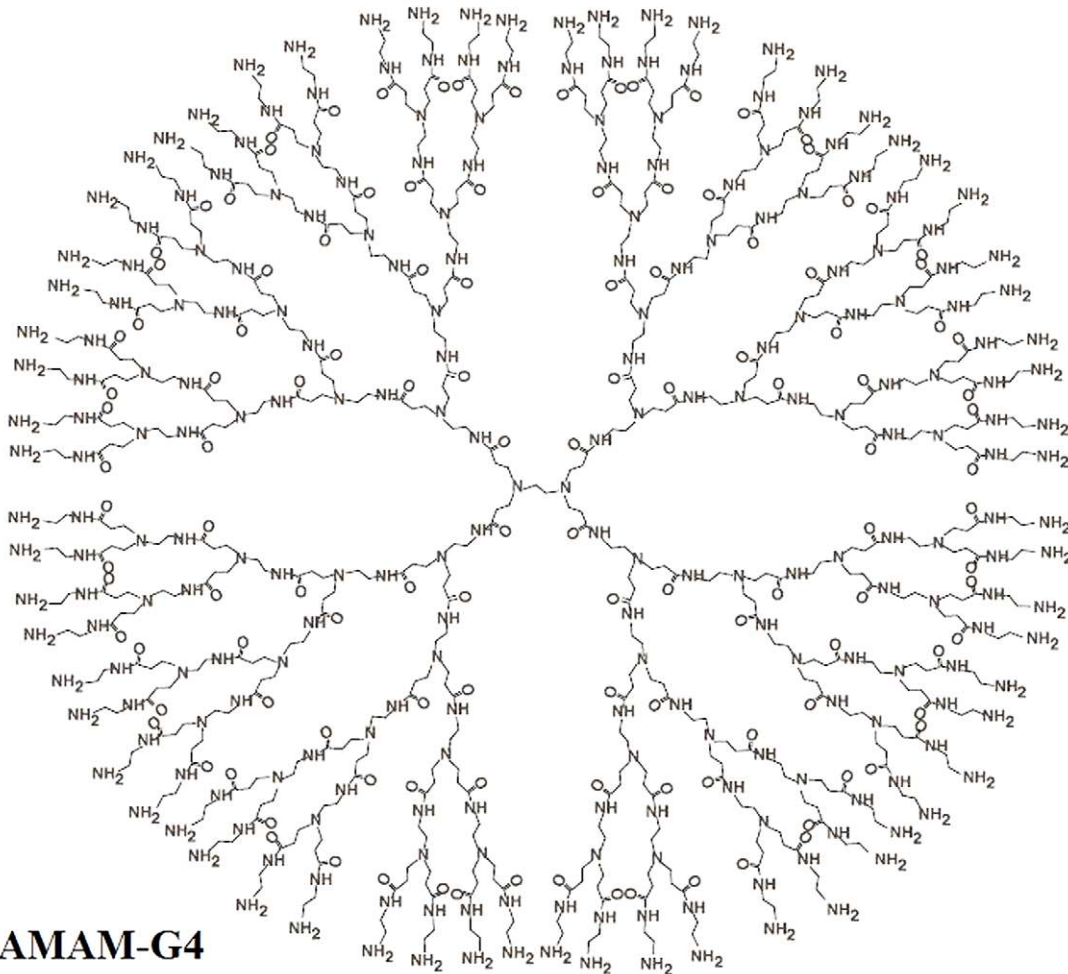


Figure 1. Chemical structures of polyamines and PAMAM-G4 dendrimer.
doi:10.1371/journal.pone.0036087.g001

combination with other substrates produces conjugated molecules, that combine the properties of both the substrate and the polymer. However, conjugate formation can alter the binding affinity of dendrimers in general since a part of the functional pendant groups are removed by conjugation.

In this report, we present the results of spectroscopic and molecular docking experiments on the interaction of biogenic and synthetic polyamines with dendrimers of different composition, PAMAM (G4), m-PEG-PAMAM (G3) and m-PEG-PAMAM (G4), in aqueous solution, using a constant polymer concentration and different drugs concentrations. Structural data regarding polyamine binding modes as well as the stability of polyamine-dendrimer complexes are presented in this report.

Materials and Methods

Materials

Spermine.4HCl and spermidine.3HCl were purchased from Sigma Chemical Company and used as supplied. Polyamine

analogues, BE-333 and BE-3333, were synthesized in the laboratory of Dr. Akira Shirahata (Josai University, Saitama, Japan). PAMAM-G4 (MW 14214 g/mol) was purchased from Aldrich Chemical Co and used as supplied. mPEG-PAMAM-G3 (MW 13423 g/mol) and mPEG-PAMAM-G4 (MW 19214 g/mol) were synthesized according to published methods [35,41,42]. mPEG block has a molecular weight of 5000 g/mol. Other chemicals were of reagent grade and used without further purification.

Preparation of stock solutions

Dendrimer solution (1 mM) were prepared in distilled water and diluted to various concentrations in Tris-HCl buffer. Polyamine solutions (1 mM) were prepared in water and diluted in Tris-HCl buffer. The pH of stock solutions was kept at 7 ± 0.2 .

FTIR spectroscopic measurements

Infrared spectra were recorded on a FTIR spectrometer (Impact 420 model), equipped with deuterated triglycine sulphate (DTGS)

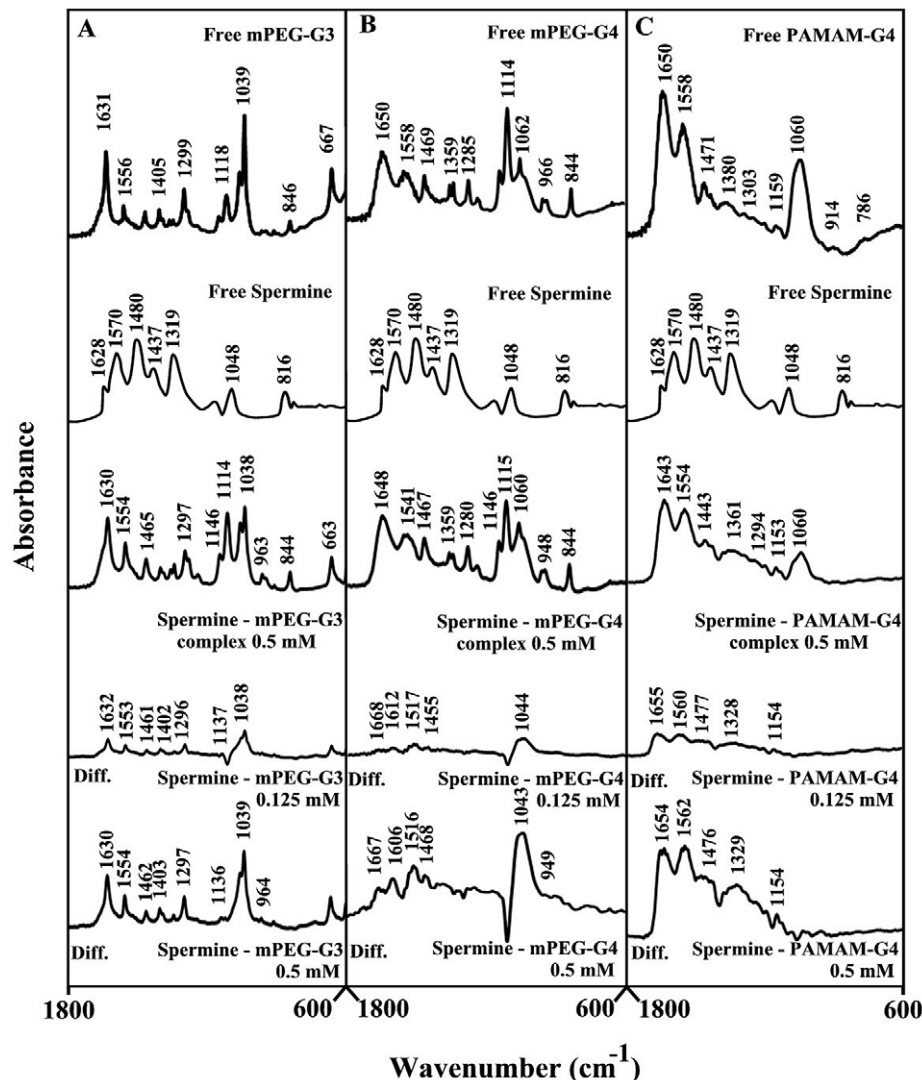


Figure 2. FTIR spectra and difference spectra (diff.) in the region of $1800\text{--}600\text{ cm}^{-1}$ of hydrated films (pH 7.4) for free mPEG-PAMAM-G3 (A), mPEG-PAMAM-G4 (B) PAMAM-G4 (C) (0.5 mM) and their spermine complexes obtained at different spermine concentrations (indicated on the figure).
doi:10.1371/journal.pone.0036087.g002

detector and KBr beam splitter, using AgBr windows. Polyamine solutions were added drop-wise to dendrimer solutions, with constant stirring to ensure the formation of homogeneous solutions and to reach target polyamine concentrations of 0.125, 0.25, and 0.5 mM and a final dendrimer concentration of 0.5 mM. Spectra were collected after 2 h incubation of polyamine and polymer solution at room temperature, using hydrated films [42]. Interferograms were accumulated over the spectral range of 4000-600 cm^{-1} , with a nominal resolution of 4 cm^{-1} and 100 scans. The difference spectra [(dendrimer+polyamine solution)–(dendrimer solution)] were generated, using dendrimer bands at 843 (mPEG-PAMAM-G3), 841 (mPEG-PAMAM-G4) and 1037 cm^{-1} (PAMAM-G4). These vibrations are related to the polymers C-C stretching and semi ring skeletal modes [43,44] that show no spectral changes (intensity or shifting) upon polyamine-dendrimer complex formation, and cancelled on spectral subtraction.

UV-Visible spectroscopy

The UV-Vis spectra were recorded on a Perkin-Elmer Lambda spectrophotometer with a slit of 2 nm and scan speed of 400 nm min^{-1} . Quartz cuvettes of 1 cm were used. The absorbance measurements were performed at pH 7.0 by keeping the concentration of dendrimer constant (0.10 mM), while increasing polyamine concentrations (0.005 mM to 0.10 mM).

The binding constants were obtained according to the method described by Connors [45]. It is assumed that the interaction between the ligand L and the substrate S is 1:1; for this reason a single complex SL (1:1) is formed. It was also assumed that the sites (and all the binding sites) are independent and all species obeyed the Beer's law. A wavelength is selected at which the molar absorptivities ϵ_s (molar absorptivity of the substrate) and ϵ_{11} (molar absorptivity of the complex) are different. In the absence of ligands and light path length (b) of 1 cm and at total substrate concentration S_0 , the solution absorbance is given by the following equation:

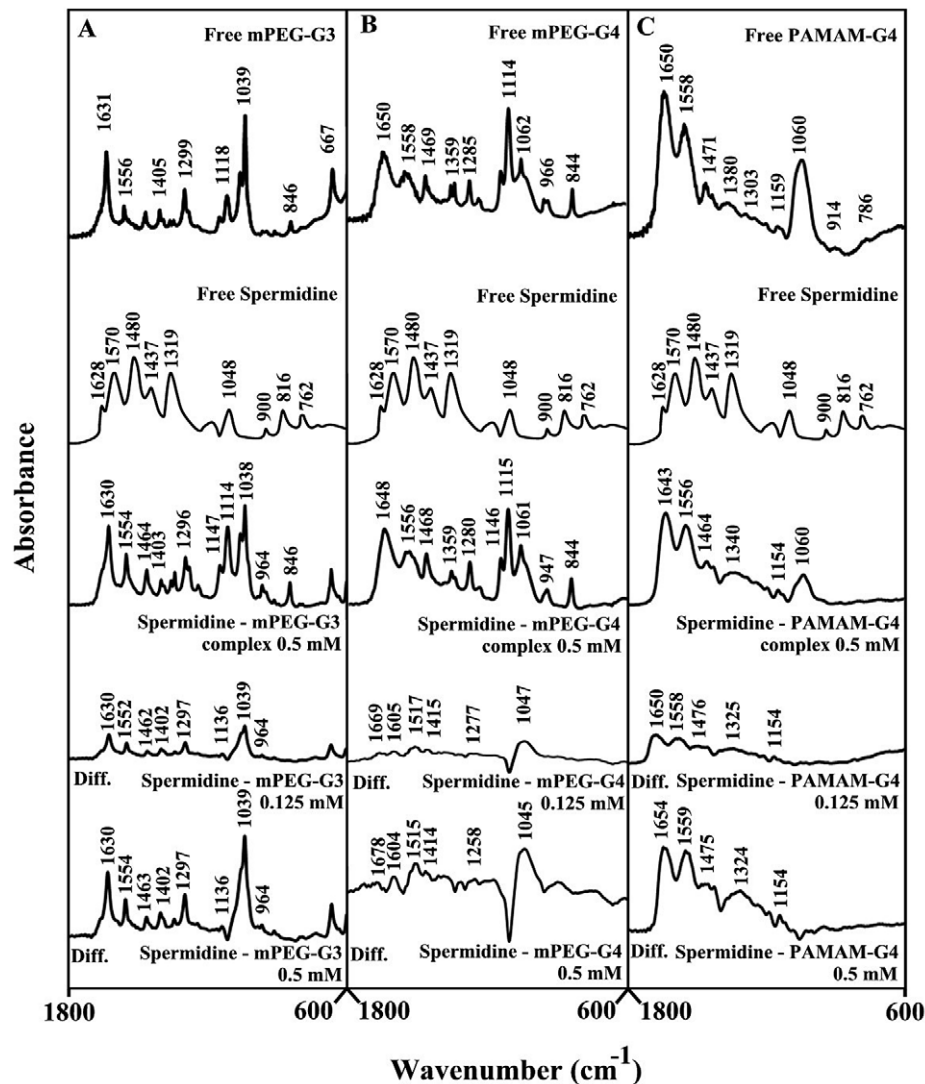


Figure 3. FTIR spectra and difference spectra (diff.) in the region of 1800-600 cm^{-1} of hydrated films (pH 7.4) for free mPEG-PAMAM-G3 (A), mPEG-PAMAM-G4 (B) PAMAM-G4 (C) (0.5 mM) and their spermidine complexes obtained at different spermidine concentrations (indicated on the figure).

doi:10.1371/journal.pone.0036087.g003

$$A_o = \epsilon_S b S_t \quad (1)$$

At total concentration L_t of a ligand, the absorbance of a solution containing the same total substrate concentration is:

$$A_L = \epsilon_S b [S] + \epsilon_L b [L] + \epsilon_{11} b [SL] \quad (2)$$

where $[S]$ is the concentration of the uncomplexed substrate, $[L]$ the concentration of the uncomplexed ligand and $[SL]$ is the concentration of the complex) which, combined with the mass balance on S and L, gives

$$A_L = \epsilon_S b S_t + \epsilon_L b L_t + \Delta \epsilon_{11} b [SL] \quad (3)$$

where $\Delta \epsilon_{11} = \epsilon_{11} - \epsilon_S - \epsilon_L$ (ϵ_L molar absorptivity of the ligand). By measuring the solution absorbance against a reference containing ligand at the same total concentration L_t , the measured

absorbance becomes

$$A = \epsilon_S b S_t + \Delta \epsilon_{11} b [SL] \quad (4)$$

Combining equation (4) with the stability constant definition $K_{11} = [SL]/[S][L]$, gives

$$\Delta A = K_{11} \Delta \epsilon_{11} b [S][L] \quad (5)$$

where $\Delta A = A - A_o$. From the mass balance expression $S_t = [S] + [SL]$ we get $[S] = S_t / (1 + K_{11}[L])$, which is equation (5), giving equation (6) at the relationship between the observed absorbance change per centimeter and the system variables and parameters.

$$\frac{\Delta A}{b} = \frac{S_t K_{11} \Delta \epsilon_{11} [L]}{1 + K_{11} [L]} \quad (6)$$

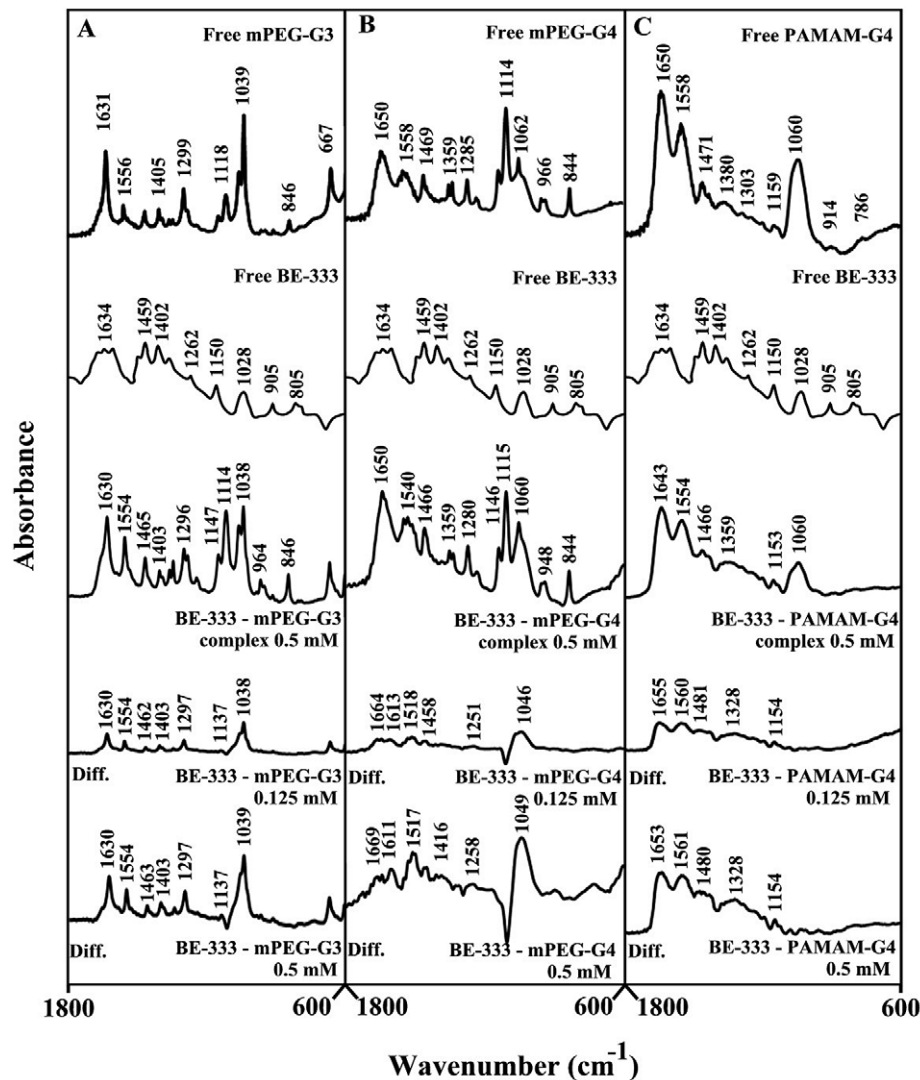


Figure 4. FTIR spectra and difference spectra (diff.) in the region of $1800\text{--}600\text{ cm}^{-1}$ of hydrated films (pH 7.4) for free mPEG-PAMAM-G3 (A), mPEG-PAMAM-G4 (B) PAMAM-G4 (C) (0.5 mM) and their BE-333 complexes obtained at different BE-333 concentrations (indicated on the figure).

doi:10.1371/journal.pone.0036087.g004

Equation (6) is the binding isotherm, which shows the hyperbolic dependence on free ligand concentration.

The double-reciprocal form of plotting the rectangular hyperbola $\frac{1}{y} = \frac{f}{d} \cdot \frac{1}{x} + \frac{e}{d}$ is based on the linearization of equation (6) according to the following equation,

$$\frac{b}{\Delta A} = \frac{1}{S_T K_{11} \Delta \varepsilon_{11} [L]} + \frac{1}{S_T \Delta \varepsilon_{11}} \quad (7)$$

Thus the double reciprocal plot of $1/\Delta A$ versus $1/[L]$ is linear and the binding constant can be estimated from the following equation

$$K_{11} = \frac{\text{intercept}}{\text{slope}} \quad (8)$$

Molecular modeling

The PAMAM-G4 and polyamine structures were generated using the ChemOffice Ultra 6.0 software suite. The polyamine was then automatically docked to the rough PAMAM-G4 structure using ArgusLab 4.0.1 (ArgusLab 4.0.1, Mark A. Thompson, Planaria Software LLC, Seattle, WA, <http://www.arguslab.com>). The docked polyamine-PAMAM-G4 structures were optimized by means of molecular dynamics using the MM+ force field available in HyperChem Pro 7.0. The heat time and run time for the simulations were 2 ps and 28 ps respectively with a step size of 0.001 ps. The temperature was initially set at 1 K and gradually increased to 300 K during the heat time by increments of 30 K. In all the simulations, equilibrium (achieving constant temperature near the selected final value) was reached after approximately 20 ps. The free binding energies of the optimized PAMAM-G4-polyamine complex structures were calculated using the Ascore scoring function provided in the ArgusLab software.

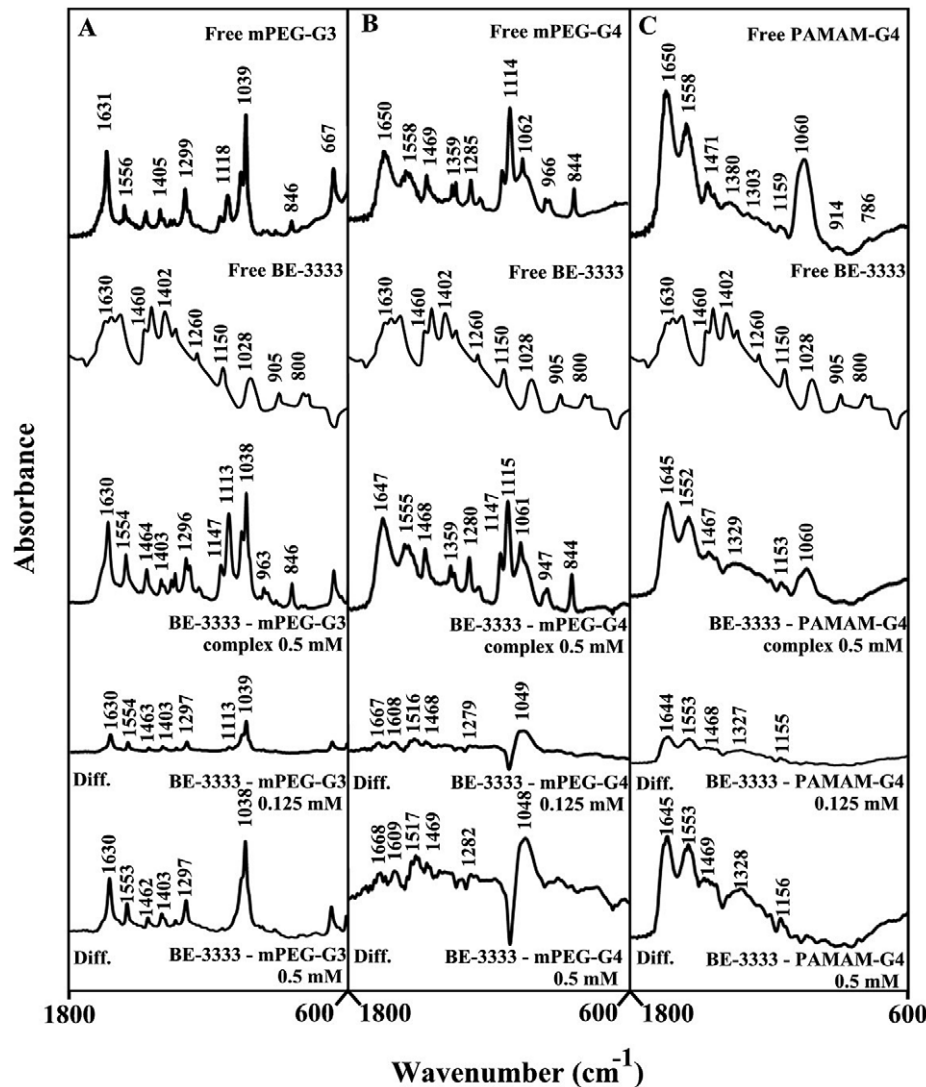


Figure 5. FTIR spectra and difference spectra (diff.) in the region of $1800\text{--}600\text{ cm}^{-1}$ of hydrated films (pH 7.4) for free mPEG-PAMAM-G3 (A), mPEG-PAMAM-G4 (B) PAMAM-G4 (C) (0.5 mM) and their BE-3333 complexes obtained at different BE-3333 concentrations (indicated on the figure). doi:10.1371/journal.pone.0036087.g005

Results

FTIR spectral analysis of polyamine-dendrimer complexes

Figure 2 shows the infrared spectra and difference spectra of dendrimers complexed with spermine. Spectral shifting was observed for the polymer C=O, C-N, C-O stretching and NH bending [43,44] due to drug hydrophilic interactions with polymer polar groups. The major infrared bands at 1631 (C=O stretch and NH bending), 1556 (C-N stretch), 1405, 1299 (C-O), 1118, 1061 and 1039 cm^{-1} (C-O and C-C stretch), in the infrared spectra of the free mPEG-PAMAM-G3 exhibited shifting and intensity increases upon spermine binding (Figs. 2A). Similarly, the major infrared bands of the free mPEG-PAMAM-G4 at 1650, 1558, 1469, 1359, 1285, 1114 and 1062 cm^{-1} showed shifting and intensity changes upon complex formation with spermine (Fig. 2 B). The infrared bands of the free PAMAM-G4 at 1650, 1558, 1471, 1380, 1159 and 1060 cm^{-1} also shifted upon spermine interaction (Fig. 2C). The observed spectral shifting was accompanied with gradual increase in intensity of the above vibrational frequencies in the difference spectra [(dendrimer+ spermine solution)–(dendrimer solution)] of drug-polymer com-

plexes (Fig. 2A, 2B and 2C, diffs). The spectral changes observed are attributed to the hydrophilic interactions of polyamine polar groups with dendrimer NH_2 , C-O and C-N groups. The hydrophilic interaction is more pronounced at high spermine concentrations as evidenced by an increase in the intensity of several positive bands, centered at 1650-1000 cm^{-1} in the difference spectra of polyamine-dendrimer complexes (Fig. 2A, 2B and 2C, compare diffs 0.125 and 0.5 mM).

Spermidine-polymer complex formation produced major spectral changes of the dendrimer infrared vibrational frequencies (Fig. 3). The spectral changes were observed mainly for the C=O, C-N, C-O stretching and NH bending modes [43,44] in the region of 1650-1000 cm^{-1} of the infrared spectra of mPEG-PAMAM-G3, mPEG-PAMAM-G4 and PAMAM-G4, upon complex formation with spermidine (Fig. 3A, 3B and 3C). The spectral shifting was associated with an increase in intensity of these vibrations in the difference spectra of spermidine-dendrimer complexes (Fig. 3A, 3B and 3C, diffs). More perturbations of polymer spectra occurred at high polyamine concentrations, as the intensity of the positive features increased as a result of spermidine-polymer complex formation (Fig. 3A, 3B and 3C. Compare diffs of

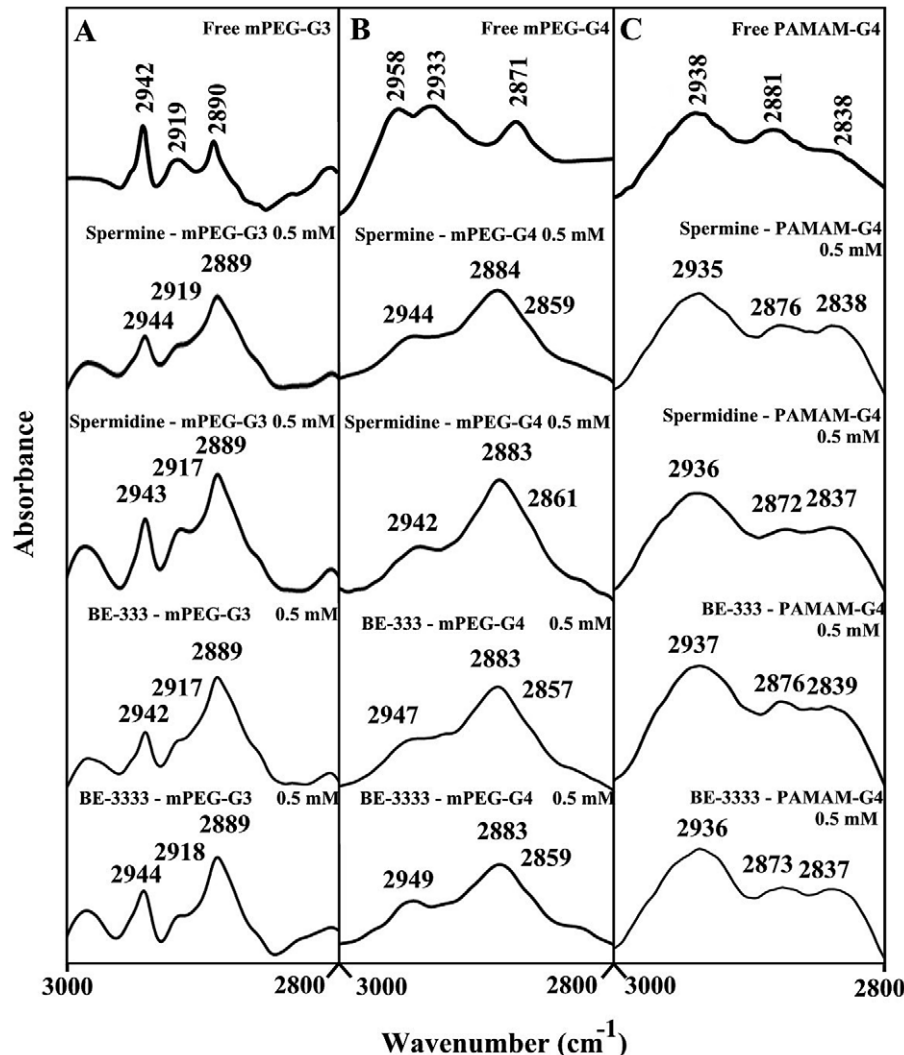


Figure 6. FTIR spectra in the region of 3300-2800 cm^{-1} of hydrated films (pH 7.4) for free mPEG-PAMAM-G3 (A), mPEG-PAMAM-G4 (B) and PAMAM-G4 (C) and their polyamine complexes obtained with 0.5 mM polymer and polyamine concentrations.

doi:10.1371/journal.pone.0036087.g006

0.125 mM and 0.50 mM). The observed spectral changes are attributed to the hydrophilic contacts of drug OH groups with dendrimer NH₂, C-O and C-N groups.

BE-333-dendrimer complexation caused minor spectral changes (shifting and intensity) at low polyamine analogue concentration, while major spectral changes occurred at high polyamine concentrations (Fig. 4A, 4B and 4C, 0.125 and 0.5 mM). The observed spectral changes (shifting and intensity increases) are due

to BE-333-polymer complex formation *via* dendrimer C-O, C-N and NH₂ and the polyamine NH₂ groups.

The infrared spectra of BE-3333-dendrimer complexes presented in Fig. 5 showed minor spectral changes at low polyamine concentration and major shifting and intensity changes at high BE-3333 concentrations (Fig. 5A, 5B, 5C, compare 0.125 and 0.5 mM). The observed spectral changes are due to polyamine-polymer interaction *via* dendrimer C-O, C-N and NH and polyamine NH₂ groups (hydrophilic contacts).

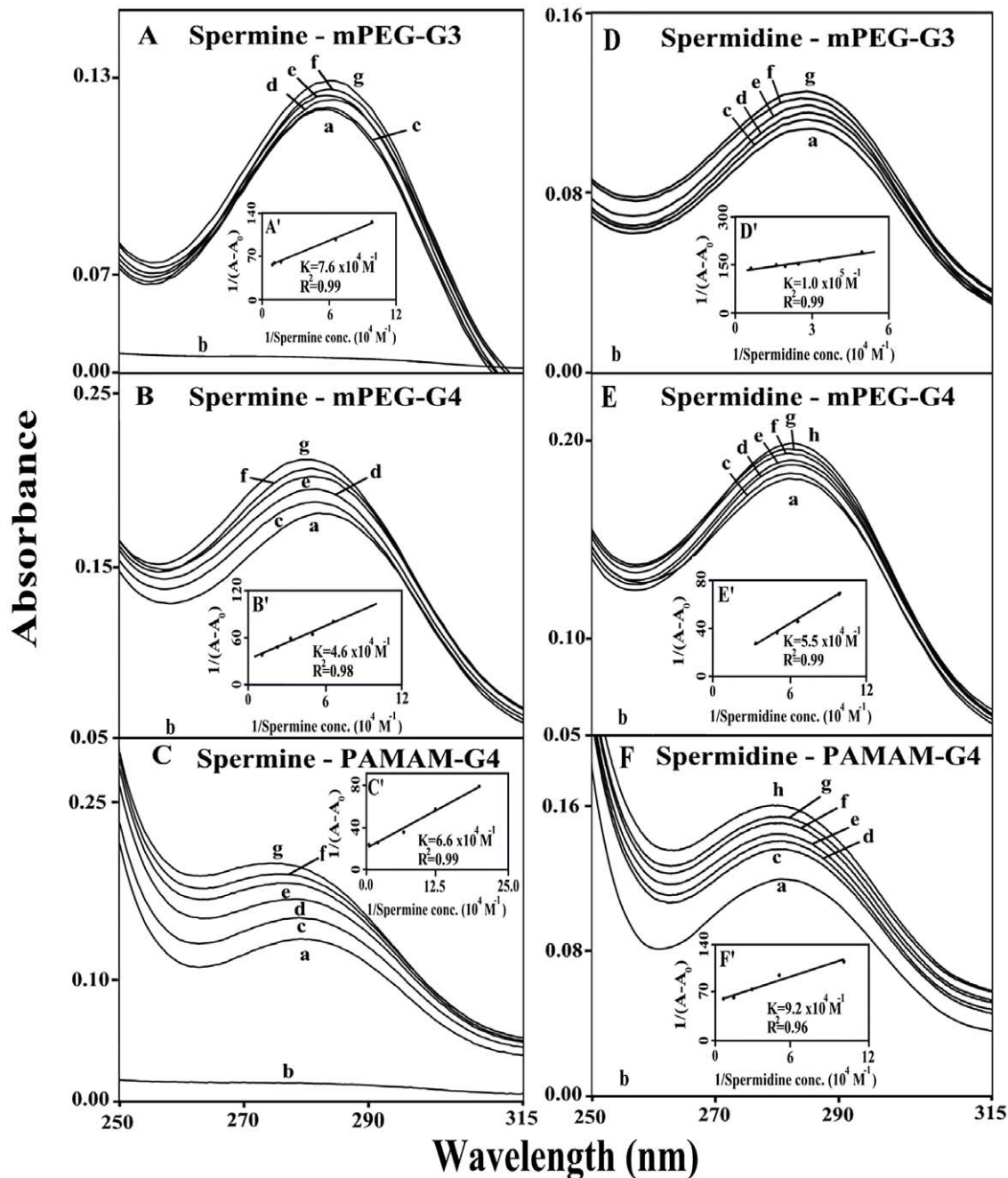


Figure 7. UV-visible spectra of mPEG-PAMAM-G3, mPEG-PAMAM-G4 and PAMAM-G4 and their complexes with spermine and spermidine with free dendrimer at 100 μM and complexes c-g at 5, 10, 20, 40 and 80 μM . (A, B and C) for spermine and c-g at 5, 10, 20, 40, and 80 μM for spermidine.mPEG-G3 (D), c-h c-g at 5, 10, 20, 40, 80 and 100 μM for spermidine-mPEG-G4 (E) and spermidine-PAMAM-G4 (F). Plots of $1/(A-A_0)$ vs $(1/\text{polyamine concentration})$ and binding constant (K) for spermine (A', B' and C') and spermidine (D', E' and F').

doi:10.1371/journal.pone.0036087.g007

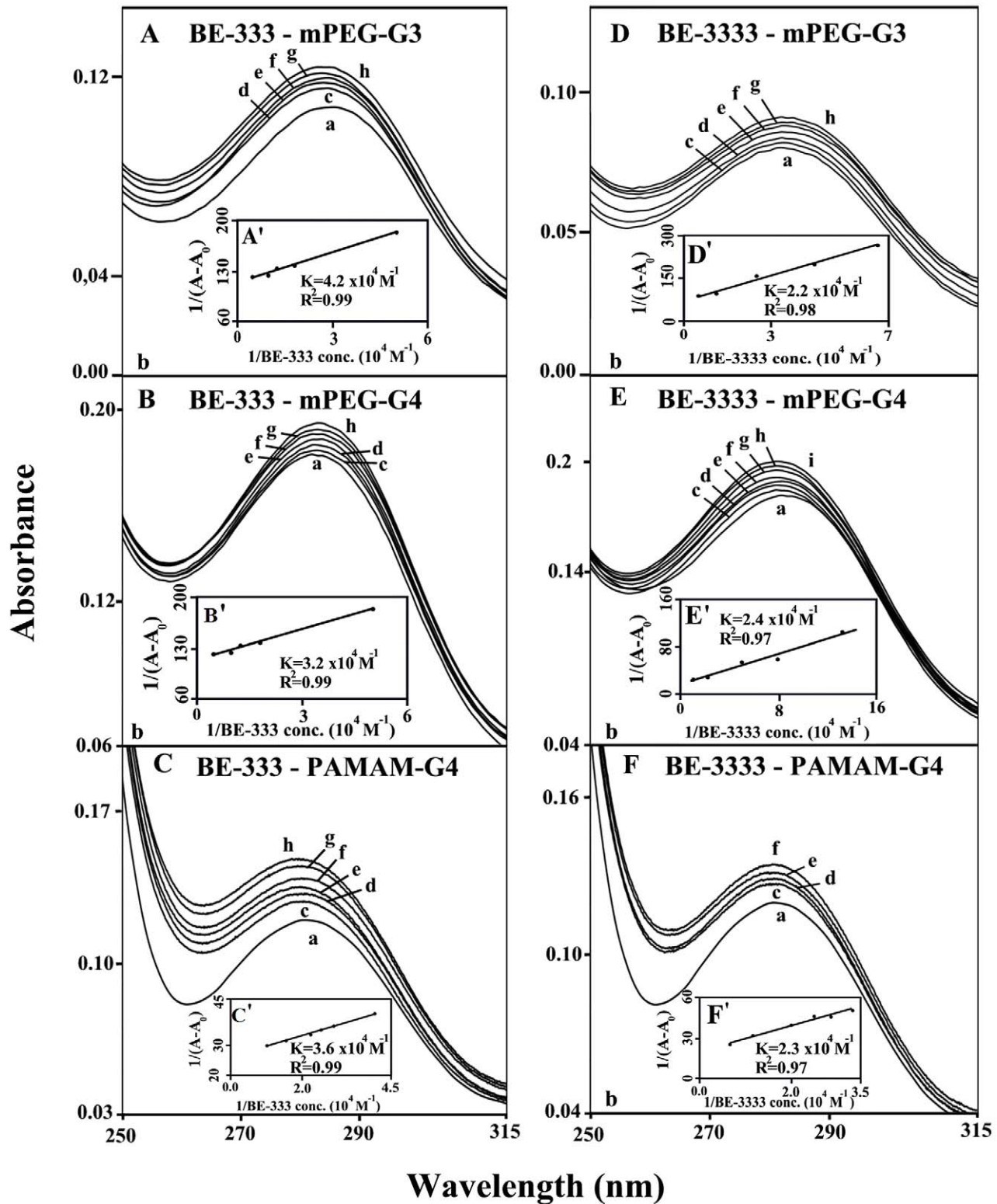


Figure 8. UV-visible spectra of mPEG-PAMAM-G3, mPEG-PAMAM-G4 and PAMAM-G4 and their complexes with BE-333 and BE-3333 with free dendrimer at 100 μM and complexes c-h at 5, 10, 20, 40, 80 and 100 μM . (A, B and C); c-h at 5, 10, 20, 40, 80 and 100 μM for BE-3333-mPEG-G3 (D), c-i at 5, 10, 20, 40, 60, 80 and 100 μM BE-3333-mPEG-G4 (E) and c-f at 5, 10, 20 and 40 μM (F). Plots of $1/(A-A_0)$ vs $1/$ polyamine concentration) and binding constant (K) for BE-333 (A', B' and C') and BE-3333 (D', E' and F').
 doi:10.1371/journal.pone.0036087.g008

Hydrophobic contacts

The effect of polyamine-polymer complex formation on dendrimer antisymmetric and symmetric CH_2 stretching vibrations in the region of $3000\text{--}2800\text{ cm}^{-1}$ was investigated by infrared spectroscopy [43,44]. From Fig. 6A, the antisymmetric and symmetric CH_2 bands of the free mPEG-PAMAM-G3 and its polyamine complexes were assigned as follows: free mPEG-PAMAM-G3 at 2942, 2912 and 2890 cm^{-1} , spermine-mPEG-PAMAM-G3 at 2944 and 2889 cm^{-1} ; spermidine-mPEG-PAMAM-G3 at 2943, 2917 and 2889 cm^{-1} ; BE-333-mPEG-PAMAM-G3 at 2942, 2917 and 2889 cm^{-1} ; and BE-3333-mPEG-PAMAM-G3 at 2944, 2918 and 2889 cm^{-1} . In Fig. 6B, the antisymmetric and symmetric CH_2 bands of the free mPEG-PAMAM-G4 and its polyamine complexes were observed as follows: mPEG-PAMAM-G4, 2958, 2933 and 2817 cm^{-1} ; spermine-mPEG-PAMAM-G4, 2944, 2984 and 2859 cm^{-1} ; spermidine-mPEG-PAMAM-G4, 2942, 2983 and 2861 cm^{-1} ; BE-333-mPEG-PAMAM-G4, 2947, 2983 and 2857 cm^{-1} ; BE-3333-mPEG-PAMAM-G4, 2949, 2983 and 2859 cm^{-1} . Similarly, Fig. 6C shows the CH_2 stretching vibrations of the free PAMAM-G4 and its complexes as follows: PAMAM-G4, 2938, 2881 and 2838 cm^{-1} ; spermine-PAMAM-G4, 2935 and 2876 cm^{-1} ; spermidine-PAMAM-G4, 2936, 2872 and 2837 cm^{-1} ; BE-333-PAMAM-G4, 2937, 2876 and 2839 cm^{-1} ; and BE-3333-PAMAM-G4, 2936, 2873 and 2837 cm^{-1} . The observed spectral shifting for polymer CH_2 vibrations is indicative of some degree of hydrophobic interactions for polyamine-dendrimer complexes. This is due to the hydrophobic contacts *via* polyamine hydrophobic parts (aliphatic CH_2 groups) and the interior hydrophobic cavities present in dendrimers.

UV-Visible spectra and stability of polyamine-dendrimer complex

The UV spectra of polyamine-dendrimer complexes are presented in Figures 7 (spermine and spermidine) and 8 (BE-333 and BE-3333). There is clear evidence that as polyamine complex formation occurred, major intensity increases of the dendrimer UV band, centered at 260–290 nm, also occurred [46,47]. The spectral changes are more pronounced in the case of biogenic spermine and spermidine than those of polyamine analogues BE-333 and BE-3333 (Figs. 7 and 8).

The polyamine-dendrimer binding constants, obtained (according to the method described in experimental section (using plots of $1/(A-A_0)$ vs $(1/\text{polyamine concentrations})$), showed one binding constant for each polyamine-polymer complex formation (Figs. 7 and 8 and Table 1). The calculated binding constants are: $K_{\text{sperm-mPEG-G3}} = 7.6 \times 10^4\text{ M}^{-1}$, $K_{\text{sperm-mPEG-PAMAM-G4}} = 4.6 \times 10^4\text{ M}^{-1}$, $K_{\text{sperm-PAMAM-G4}} = 6.6 \times 10^4\text{ M}^{-1}$, $K_{\text{sperm-d-mPEG-G3}} = 1.0 \times 10^5\text{ M}^{-1}$, $K_{\text{sperm-d-mPEG-PAMAM-G4}} = 5.5 \times 10^4\text{ M}^{-1}$, $K_{\text{sperm-d-PAMAM-G4}} = 9.2 \times 10^4\text{ M}^{-1}$, $K_{\text{BE-333-mPEG-G3}} = 4.2 \times 10^4\text{ M}^{-1}$, $K_{\text{BE-333-mPEG-PAMAM-G4}} = 3.2 \times 10^4\text{ M}^{-1}$, $K_{\text{BE-333-PAMAM-G4}} = 3.6 \times 10^4\text{ M}^{-1}$, $K_{\text{BE-3333-mPEG-G3}} = 2.2 \times 10^4\text{ M}^{-1}$, $K_{\text{BE-3333-mPEG-PAMAM-G4}} = 2.4 \times 10^4\text{ M}^{-1}$, $K_{\text{BE-3333-PAMAM-G4}} = 2.3 \times 10^4\text{ M}^{-1}$ (Table 1). The binding affinity of biogenic polyamines toward dendrimers was stronger than that of synthetic polyamines, while weaker interaction was observed as polyamine cationic charge increased (Table 1). The reason why biogenic polyamine-dendrimers are more stable than those of the synthetic polyamines can be due to other factors such as the primary amines (NH_3^+) in biogenic polyamines, that possess a higher density of positive charge than the secondary ones (NH_2^+), in synthetic polyamines and also the presence of more hydrophobic contacts in the biogenic polyamine-polymer complexes.

Table 1. Binding constants of polyamine-dendrimers ($K\text{ M}^{-1}$).

Polyamines	mPEG-G3	mPEG-G4	PAMAM-G4
Spermine	$(7.6 \pm 1) \times 10^4$	$(4.6 \pm 0.6) \times 10^4$	$(6.6 \pm 1) \times 10^4$
Spermidine	$(1 \pm 0.4) \times 10^5$	$(5.5 \pm 0.7) \times 10^4$	$(9.2 \pm 1) \times 10^4$
BE-333	$(4.2 \pm 0.6) \times 10^4$	$(3.2 \pm 0.5) \times 10^4$	$(3.6 \pm 0.6) \times 10^4$
BE-3333	$(2.2 \pm 0.5) \times 10^4$	$(2.4 \pm 0.4) \times 10^4$	$(2.3 \pm 0.4) \times 10^4$

doi:10.1371/journal.pone.0036087.t001

Docking studies

Our results from FTIR and UV-visible spectroscopic methods were complemented with molecular dynamic simulations in which the polyamines spermine, spermidine and BE-333 were automatically docked to PAMAM-G4 and the resulting structures were optimized using the MM+ force field to determine the preferred conformations of the polyamine-polymer complexes. The simulation results are shown in Fig. 9 and Table 2. The models showed that polyamines are located on the surface of dendrimers and in cavities of PAMAM-G4 polymer (Fig. 9). The free binding energies calculated from docking studies were as follows: spermine, (3.2); spermidine, (3.5) and BE-333, (3.03) kcal/mol, with the following order of binding affinity: spermidine-PAMAM-G4 > spermine-PAMAM-G4 > BE-333-PAMAM-G4. These results are consistent with the data obtained from spectroscopic studies (Tables 1 and 2).

Discussion

Several synthetic macromolecules have been developed as drug and gene delivery vehicles [27,28,30,32]. An ideal drug carrier vehicle must be biochemically inert and non-toxic, while protecting the payload (drug) from dissociation until it reaches the target site, and capable of releasing the drug at target site. Among synthetic polymers, dendrimers are unique macromolecules with nanometer dimensions, a highly branched structure and globular shape. These macromolecules have uniform size and are mono-disperse, with modifiable surface functionality as well as internal cavities. They contain several binding sites for hydrophobic, hydrophilic, cationic and anionic drugs (Fig. 1) Dendrimers are capable of binding and transporting DNA, RNA and drug molecules with high efficiency [30,32]. Dendrimers can be used as containers to encapsulate drug molecules and carry them to different targets *in vivo* [35,48,49]. It has been shown that dendrimers with a hydrophobic interior and hydrophilic chain ends are capable of solubilizing hydrophobic compounds in aqueous solutions [49,50,51]. Attempts have been made to design different dendrimers as drug carriers [36]. For example, anticancer drug, 5-fluorouracil (5-FU) was attached to dendrimers with cyclic core [36]. Dendrimers having poly(ethylene glycol)

Table 2. Free binding energy of the docked polyamine-PAMAM complexes.

Complex	$\Delta G_{\text{binding}}$ (kcal/mol)
Spermidine – PAMAM-G4	–3.50
Spermine – PAMAM-G4	–3.20
BE-333 – PAMAM-G4	–3.03

doi:10.1371/journal.pone.0036087.t002

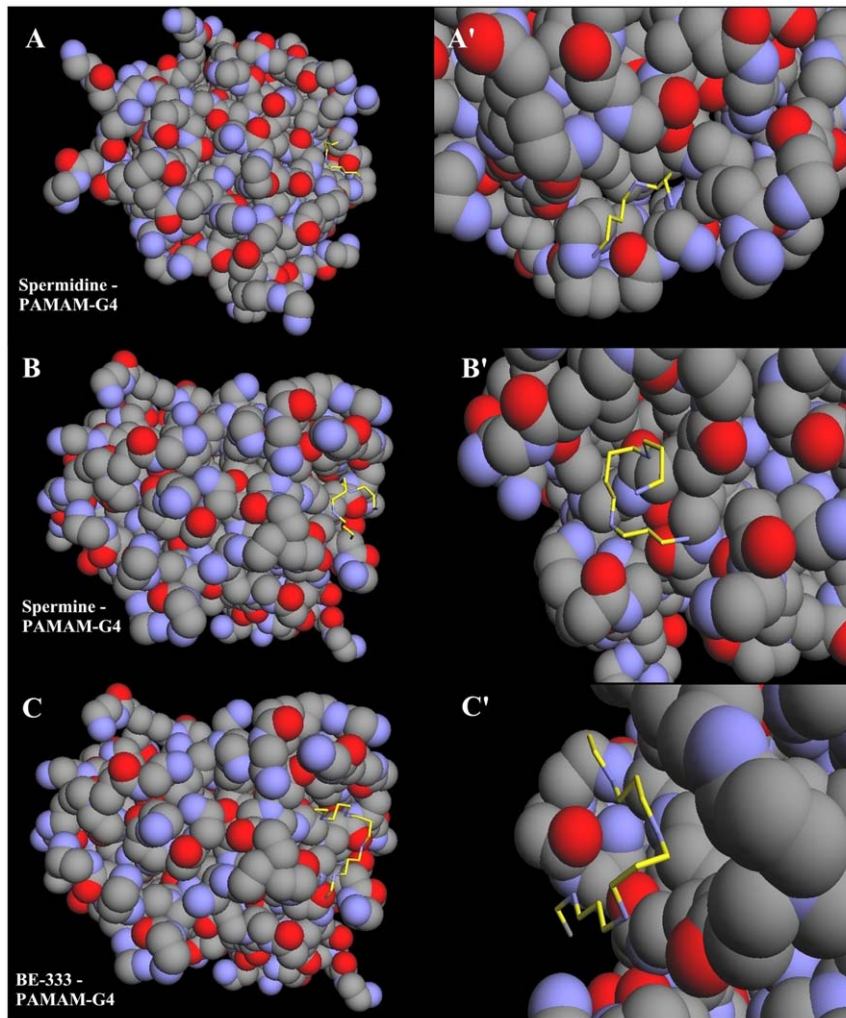


Figure 9. Optimized polyamine-PAMAM-G4 docking structures. The polyamines are shown in yellow color. (A) shows whole PAMAM-G4 in spheres with spermine and (A') shows the zoom on the binding site represented in sticks. (B) shows whole PAMAM-G4 in spheres with spermidine and (B') shows the binding site represented in sticks. (C) whole PAMAM-G4 in spheres with BE-333 and (C') shows the binding site in represented in sticks.

doi:10.1371/journal.pone.0036087.g009

grafts have been used to encapsulate antitumor drugs adriamycin and methotrexate [37]. The complexation of dendrimers with anti-inflammatory drug flurbiprofen was studied *in vitro* and *in vivo*, while drug biodistribution in different organs has been monitored [39]. Gene delivery targeted to brain has been attempted using transferring-conjugated polyethyleneglycol-modified polyamidoamine dendrimer [40]. The purpose of our investigation was to analyze the interaction of dendrimers with biogenic and synthetic polyamines in order to test the feasibility of these nanocarrier molecules for polyamine-based drug delivery. Infrared spectroscopic data in the region of $1700\text{-}1000\text{ cm}^{-1}$, where most of the polymer in-plane vibrations related to C=O, C-N, NH and C-O modes are located, exhibit spectral changes (shifting and intensity variations) upon polyamine-polymer complex formation. These changes are more profound at high polyamine concentrations. There was clear evidence that the hydrophilic polyamine entity induced more perturbations of polymer hydrophilic group vibrational frequencies, with the following order of spectral changes: spermidine>spermine>BE-

333>BE-3333 (Figs. 2, 3, 4, 5). This can be expected since polyamines with several positively charged NH and NH_2 groups show more affinity for dendrimer terminal groups than those of the hydrophobic groups located in polymer interior cavities. Molecular modeling also showed polyamine binding with the dendrimer with spermidine-PAMAM more stable than spermine- and BE-333-PAMAM complexes.

In conclusion, we find that synthetic and natural polyamines are capable of binding to different dendrimers. The binding affinity is relatively low to enable them to act as polyamine delivery vehicles, especially polyamine analogues under investigation as cancer chemotherapeutic agents.

Author Contributions

Conceived and designed the experiments: JSM PB TJJ HATR. Performed the experiments: JSM PB TJJ. Analyzed the data: JSM PB. Contributed reagents/materials/analysis tools: TJ. Wrote the paper: HATR.

References

- Huang Y, Keen JC, Pledge A, Marton LJ, Zhu T, et al. (2006) Polyamine analogues down-regulate estrogen receptor α expression in human breast cancer cells. *J Biol Chem* 281: 19055–19063.
- Huang Y, Keen JC, Hager E, Smith R, Hacker A, et al. (2004) Regulation of polyamine analogue cytotoxicity by c-jun in human MDA-MB-435 cancer cells. *Mol Cancer Res* 2: 81–88.
- Casero RA, Woster PM (2001) Terminally alkylated polyamine analogues as chemotherapeutic agents. *J Med Chem* 44: 1–26.
- Gerner EW, Meyskens FL (2004) Polyamines and cancer: old molecules, new understanding. *Nat Rev Cancer* 4: 781–792.
- Bergeron RJ, Neims AT, McManis JS, Hawthorne TR, Vinson JRT, et al. (1988) Synthetic polyamines analogues as antineoplastics. *J Med Chem* 31: 1183–1190.
- Bergeron RJ, McManis JS, Liu CZ, Frng Y, Weimar WR, et al. (1994) Antiproliferative properties of polyamine analogues: a structure-activity study. *J Med Chem* 37: 3464–3476.
- Davidson NE, Mank AR, Prestigiacomo LJ, Bergeron JR, Casero RA (1993) Growth inhibition of hormone-responsive and resistant human breast cancer cells in culture by N^1, N^{12} -bis (ethyl)spermine. *Cancer Res* 53: 2071–2075.
- Thomas T, Balabhadrapathruni S, Gallo MA, Thomas TJ (2002) Development of polyamine analogues as cancer therapeutic agents. *Oncol Res* 13: 123–135.
- Faaland CA, Thomas TJ, Balabhadrapathruni S, Langer T, Mian S, et al. (2000) Molecular correlates of the action of bis(ethyl)polyamines in breast cancer cell growth inhibition and apoptosis. *Biochem Cell Biol* 78: 415–426.
- Thomas T, Thomas TJ (2003) Polyamine metabolism and cancer. *J Cell Mol Med* 7: 113–126.
- McCloskey DE, Pegg AE (2003) Properties of the spermidine/spermine N^1 -acetyltransferase mutant L156F that decreases cellular sensitivity to the polyamine analogue N^1, N^{12} -bis(ethyl)nospermine. *J Biol Chem* 278: 13881–13887.
- Ha HC, Woster PA, Yager JD, Castro RA (1997) The role of polyamine catabolism in polyamine analogue-induced programmed cell death. *Proc Natl Acad Sci USA* 94: 11557–11562.
- Ha HC, Sirisoma NS, Kuppasamy P, Zweier LJ, Woster PM, et al. (1998) The natural polyamines spermine functions directly as a free radical scavenger. *Proc Natl Acad Sci U S A* 95: 11140–11145.
- Tabor CW, Tabor H (1984) Polyamines. *Annu Rev Biochem* 53: 749–790.
- Pegg AE (1988) Polyamine metabolism, and its importance in neoplastic growth and a target of chemotherapy. *Cancer Res* 48: 759–774.
- Heby O (1981) Role of polyamines in the control of cell proliferation and differentiation. *Differentiation* 19: 1–20.
- Tkachenko AG, Nesterova LY (2003) Polyamines as modulators of gene expression under oxidative stress in *Escherichia coli*. *Biochemistry (Moscow)* 68: 850–856.
- Marton LJ, Pegg AE (1995) Polyamines as targets for therapeutic intervention. *Annu Rev Pharmacol Toxicol* 35: 55–91.
- Cohen SS (1998) A Guide to the polyamines, Oxford Uni. Press, New York.
- Thomas T, Thomas TJ (2001) Polyamine in cell growth and death. *Cell Mol Life Sci* 58: 244–258.
- Ahmed Ouameur A, Tajmir-Riahi HA (2004) Structural analysis of DNA interactions with biogenic polyamines and cobalt (III) hexamine studied by Fourier transform infrared and capillary electrophoresis. *J Biol Chem* 279: 42041–42050.
- Ahmed Ouameur A, Bourassa P, Tajmir-Riahi HA (2010) Probing tRNA interaction with biogenic polyamines. *RNA* 16: 1968–1979.
- N'soukpoé-Kossi CN, Ahmed Ouameur A, Thomas T, Shirahata A, Thomas TJ, et al. (2008) DNA interaction with antitumor polyamine analogues: A comparison with biogenic polyamines. *Biomacromolecules* 9: 2712–2718.
- N'soukpoé-Kossi CN, Ahmed Ouameur A, Thomas T, Thomas TJ, Tajmir-Riahi HA (2009) Interaction tRNA with antitumor polyamine analogues. *Biochem Cell Biol* 87: 621–630.
- D'Agostino L, di Pietro M, Di Luccia A (2005) Nuclear aggregates of polyamines are supramolecular structures that play a crucial role in genomic DNA protection and conformation. *FEBS J* 272: 3777–3787.
- Hardy JG, Mauri A, David K, Smith K, Gabrielson NP, et al. (2006) Dendrons with spermine surface groups as potential building blocks for nonviral vectors in gene therapy. *Bioconjugate Chem* 17: 172–178.
- Galeazzi S, Hermans TM, Paolino M, Anzini M, Mennuni L, et al. (2010) Multivalent supramolecular dendrimer-based drugs. *Biomacromolecules* 11: 182–186.
- Hu J, Fang M, Cheng Y, Zhang J, Wu Q, et al. (2010) Host-guest chemistry of dendrimer-drug complexes. 4. An in depth look into the binding/encapsulation of guanosine monophosphate by dendrimers. *J Phys Chem B* 114: 7148–7157.
- Maiti PK, Caing T, Wang G, Goddard WA (2004) Structure of PAMAM dendrimers: Generations 1 through 11. *Macromolecules* 37: 6236–6254.
- Patri AK, Majoros JJ, Baker JR (2002) Dendritic polymer macromolecular carriers for drug delivery. *Curr Opin Chem Biol* 6: 466–471.
- Tomilia DA (2005) Birth of a new macromolecular architecture: dendrimers as quantized building blocks for nanoscale synthetic polymer chemistry. *Prog Polymer Sci* 30: 294–324.
- Klajnert B, Bryszewska M (2007) Dendrimers as delivery systems in gene therapy; in: New developments in mutation research Valon CL, ed. Chapter 9. pp 217–240.
- Lee CC, Mackay JA, Fréchet JM, Szoka FC (2005) Designing dendrimers for biological applications. *Nature Biotech* 23: 1517–1526.
- Klajnert B, Bryszewska M (2007) in: Dendrimers in Medicines Klajnert B, Bryszewska M, eds. Nova Science publisher, Inc., New York.
- Kojima C, Kono K, Maruyama K, Takagishi T (2000) Synthesis of polyamidoamine dendrimers having poly(ethylene glycol) grafts and their ability to encapsulate anticancer drugs. *Bioconjugate Chem* 11: 910–917.
- Zhuo RX, Du B, Lu ZR (1999) In vitro release of 5-fluorouracil with cyclic core dendritic polymer. *J Control Release* 57: 249–257.
- Kono K, Liu M, Fréchet JM (1999) Design of dendritic macromolecules containing folate or methotrexate residues. *Bioconjugate Chem* 10: 1115–1121.
- Jansen JFGA, Meijer EW, de Brabander-van den Berg EMM (1995) The dendritic box: shape-selective liberation of encapsulated guests. *J Am Chem Soc* 117: 4417–4418.
- Malik N, Wiwattanapatapee R, Klopsch R, Lorenz K, Frey H, et al. (2000) Dendrimers: relationship between structure and biocompatibility in vitro, and preliminary studies on the biodistribution of 125I-labeled poly (amido amine) dendrimers in vivo. *J Control Release* 65: 133–148.
- Jevprascaphant R, Penny J, Jalal R, Atwood D, McKown N, et al. (2000) The influence of surface modifications on the cytotoxicity of PAMAM dendrimers. *Int J Pharm* 252: 263–266.
- Iyer J, Fleming K, Hammond PT, Paula TH (1998) Synthesis and solution properties of new linear-dendritic diblock copolymers. *Macromolecules* 31: 8757–8765.
- Froehlich E, Mandeville JS, Weinert CM, Kreplak L, Tajmir-Riahi HA (2011) Bundling and aggregation of DNA by cationic dendrimers. *Biomacromolecules* 12: 511–517.
- Popescu MC, Filip D, Vasile C, Cruz C, Rueff JM, et al. (2006) Characterization by Fourier transform infrared spectroscopy (FT-IR) and 2D IR correlation spectroscopy of PAMAM dendrimer. *J Phys Chem B* 110: 14198–14211.
- Singh P, Gupta U, Asthana A, Jain NK (2008) Folate and folate-PEG-PAMAM dendrimers: synthesis, characterization, and targeted anticancer drug delivery potential in tumor bearing mice. *Bioconjugate Chem* 19: 2239–2252.
- Connors K. Binding constants: The measurement of molecular complex stability, John Wiley & Sons, New York.
- Dubeau S, Bourassa P, Thomas TJ, Tajmir-Riahi HA (2010) Biogenic and synthetic polyamines bind bovine serum albumin. *Biomacromolecules* 11: 1507–1515.
- Esseminea J, Hasnia I, Carpentiera R, Thomas TJ, Tajmir-Riahi HA (2011) Binding of biogenic and synthetic polyamines to beta-lactoglobulin. *Int J Biol Macromol* 49: 201209.
- Jansen JFGA, Meijer EW, de Brabander-van den Berg EMM (1994) Encapsulation of guest molecules into a dendritic box. *Science* 266: 1226–1229.
- Hawke CJ, Wooley KL, Fréchet JM (1999) Unimolecular micelles and globular amphiphiles; dendritic macromolecules as novel recyclable solubilization agents. *J Chem Soc Perkin Trans.* pp 1287–1297.
- Twyman IJ, Beezer AE, Esfand R, Dardy MJ, Michell JC (1999) The synthesis of water soluble dendrimers and their application as possible drug delivery systems. *Tetrahedron Lett* 40: 1743–1746.
- Abderrezak A, Bourassa P, Mandeville JS, Sedaghat-Herati R, Tajmir-Riahi HA (2012) Dendrimers bind antioxidant polyphenols and cisplatin drug. *PLoS ONE* 7: e33102, 1–12.